Localization of Nonspecific Lipid Transfer Proteins Correlate with Programmed Cell Death Responses during Endosperm Degradation in *Euphorbia lagascae* Seedlings[1]

D. Magnus Eklund and Johan Edqvist*

Department of Plant Biology and Forest Genetics, Swedish University of Agricultural Sciences, Box 7080, 750 07 Uppsala, Sweden

When the storage materials have been depleted, the endosperm cells undergo programmed cell death. Very little is known about how the components of the dying cells are recycled and used by the growing seedling. To learn more about endosperm degradation and nutrient recycling, we isolated soluble proteins from the endosperm of *Euphorbia lagascae* seedlings collected 2, 4, and 6 d after sowing. The protein extracts were subjected to two-dimensional gel electrophoresis. Proteins that increased in amount in the endosperm with time were selected for further analysis with mass spectrometry. We successfully identified 17 proteins, which became more abundant by time during germination. Among these proteins were three *E. lagascae* lipid transfer proteins (ElLTPs), ElLTP1, ElLTP2, and ElLTP3. Detailed expressional studies were performed on ElLTP1 and ElLTP2. ElLTP1 transcripts were detected in endosperm and cotyledons, whereas ElLTP2 transcripts were only detected in endosperm. Western blots confirmed that ElLTP1 and ElLTP2 accumulate during germination. Immunolocalization experiments showed that ElLTP1 was present in the vessels of the developing cotyledons, and also in the alloplastic space in the endosperm. ElLTP2 formed a concentration gradient in the endosperm, with higher amounts in the inner regions close to the cotyledons, and lesser amounts in the outer regions of the endosperm. On the basis of these data, we propose that ElLTP1 and ElLTP2 are involved in recycling of endosperm lipids, or that they act as protease inhibitors protecting the growing cotyledons from proteases released during programmed cell death.

The endosperm is a tissue that is destined to be degraded, so when the storage materials are depleted, the cells of the endosperm undergo senescence by programmed cell death (PCD; Schmid et al., 1999). In senescing tissues, the degree of processing of dead and dying cells ranges from that apparently limited to the nucleus or nDNA to complete autolysis. One important route for recycling of proteins is vacuolar autophagy, which takes place during starvation and PCD (Reggiori and Klionski, 2002). In autophagy in yeasts, a portion of the cytoplasm is enclosed by the autophagosome, which is a double-membraned structure. The autophagosome then fuses to the vacuole, where the cytoplasmic contents are degraded. The system is similar in animal cells, although here the lysosome acts as the degrading compartment. One of the essential components of the autophagic system in yeasts is a pair of conjugation pathways that attach polypeptide tags to the lipid phosphatidylethanolamine and the protein APG8 (Ichimura et al., 2000). By an unknown mechanism, these modifications trigger autophagosome assembly and fusion of the vesicles with the vacuole.

There is probably a similar system for autophagy in plant tissues, because the genome of Arabidopsis contain at least 25 APG genes that are homologous to yeast genes essential for autophagy. Interestingly, leaf senescence was shown to accelerate in Arabidopsis lacking a functional gene for APG9 (Hanaoka et al., 2002). Premature leaf senescence was also observed in Arabidopsis plants having a disrupted APG7 (Doelling et al., 2002). Thus, there seems to be a need for autophagy during certain situations that require substantial nitrogen and carbon mobilization, such as leaf senescence. It has also been shown that a long period of Suc starvation induced autophagy in suspension cultures of *Acer* spp. cells (Aubert et al., 1996). In this case, autophagy was paralleled with a massive breakdown of membrane lipids.

It is not known whether autophagy or other cellular activities are involved in the degradation and recycling of cellular components from senescing endosperm cells. Previously, we observed that transcription of nonspecific lipid transfer proteins (LTPs) was induced during germination, and we suggested that LTPs may be involved in the recycling of lipids from senescing endosperm cells (Edqvist and Farbos, 2002). LTPs are characterized by their structure and ability to enhance the in vitro exchange of various polar lipids between different membranes (Kader, 1996; Kader et al., 1984). The primary structure of LTP is generally 90 to 95 amino acids, not including

[1] This work was supported by the Carl Trygger Foundation, by the Magnus Bergvall Foundation, and by the AgriFunGen Research Program in Functional Genomics at Swedish University of Agricultural Sciences.

* Corresponding author; e-mail Johan.Edqvist@vbsg.slu.se; fax 46–18–673279.

Article, publication date, and citation information can be found at www.plantphysiol.org/cgi/doi/10.1104/pp.103.020875.

the N-terminal signal peptide directing the protein to the apoplastic space (Tchang et al., 1988). The three-dimensional structure has been determined for LTPs from many species such as rice (*Oryza sativa*; Lee et al., 1998), maize (*Zea mays*; Gomar et al., 1996), and barley (*Hordeum vulgare*; Heinemann et al., 1996) and reveals a very compact structure consisting of four α-helices tightly connected by eight Cys residues forming four sulfide bridges. The four helices form a hydrophobic cavity, which is the binding site for fatty acids, acyl-CoA, or phospholipids (Lee et al., 1998). The cavity can adapt its volume to bind one or two monoacyl lipids, diacylated lipids, or a wide variety of hydrophobic molecules (Douliez et al., 2000, 2001). When the interaction between a wheat (*Triticum aestivum*) LTP and phospholipids was studied using the monolayer technique, it was shown that the incorporation of the LTP within the lipid monolayers was surface pressure dependent (Subirade et al., 1995). This finding may indicate that LTPs cannot load lipids from intact membranes under normal physiological conditions (Blein et al., 2002).

LTPs are not specified to any certain tissue or organ, instead they have been found in various tissues throughout the whole plant but in some tissues only at certain developmental stages. For example, LTPs have been found in potato (*Solanum tuberosum*) tubers (Horvath et al., 2002), in the epicuticular waxy layer of broccoli (Pyee et al., 1994), and in the epidermal cells of Arabidopsis (Thoma et al., 1994), during formation of vascular tissues (Endo et al., 2001) and during pathogen attack (Segura et al., 1993; Garcia-Olmedo et al., 1995). These findings provide suggestions on the biological function, or functions, of LTPs in plant tissues, but so far no biological role has been firmly established. LTPs are thought to be involved in processes like formation and reinforcement of plant surface layers (Sterk et al., 1991) and in defense against pathogens (Garcia-Olmedo et al., 1995). LTPs are also reported to serve as anti-microbial factors (Cammue et al., 1995) perhaps functioning as an elictin antagonist (Buhot et al., 2001). Recently, it was also shown that LTP may be involved in systemic resistance signaling (Maldonado et al., 2002).

To learn more about endosperm degradation and recycling and to elucidate the role of LTPs in such processes, we decided to follow the development of the endosperm proteome of *Euphorbia lagascae* during germination. In *E. lagascae*, the endosperm contain high amounts of the epoxidated fatty acid vernolic acid, which has potential industrial usages in paint, coating, and lubricant production as an alternative to petroleum derived oils. Our research interest was originally on enzymes participating in the metabolism of vernolic acid during seed germination (Edqvist and Farbos, 2002, 2003). But we have also recognized that the large size of the *E. lagascae* seeds make them attractive for proteomic and biochemical studies in relation to endosperm depletion. In this report, we describe that the *E. lagascae* LTPs ElLTP1, ElLTP2, and ElLTP3 are accumulating in the endosperm during seed germination. We also present a detailed protein expression analysis of ElLTP1 and ElLTP2. On the basis of our obtained results we propose that ElLTP1 and ElLTP2 are involved in recycling of endosperm lipids or that they act as protease inhibitors protecting the growing cotyledons from proteases released during PCD.

RESULTS

Endosperm Morphology of Germinating *E. lagascae* Seedlings

The seed structure of *E. lagascae* resembles very much that of castor bean (*Ricinus communis*), a well-established model organism for studies on seed germination (Beevers, 1980). In these seeds, there are no specialized digestive tissues, so the oils and proteins are stored in a living endosperm laterally attached to the cotyledons. During germination, the cotyledons are carried above ground by the elongating hypocotyl. In *E. lagascae*, the elongating hypocotyl forms a hook, which straightens out and pulls the cotyledons together with the endosperm and seed coat above ground. The seed coat ruptures on d 0 to 1 after sowing in moist vermiculite, and the radicle emerges on d 1 to 2 (Fig. 1A). Four days after sowing, the endosperm has become more oval-shaped and elongated (Fig. 1B), and the hypocotyl is starting to reach above ground. On d 6, a thin dry mantle encloses the remaining endosperm as well as the cotyledons (Fig. 1C). Seven to 8 d after sowing, the last remains of the endosperm is consumed and as the dry mantle ruptures the cotyledons are separated. The growth of the hypocotyl is rapid (Fig. 1D), whereas the loss of fresh weight from the endosperm tissues starts approximately 4 d after sowing (Fig. 1E).

Proteome Analysis

To identify proteins involved in endosperm degradation, we extracted proteins from the endosperm at 2, 4, and 6 d of germination. The protein extracts were precipitated with TCA and analyzed by two-dimensional gel electrophoresis (Fig. 2). The 2-, 4-, and 6-d proteomes can easily be told apart by the pattern of proteins with a molecular mass of approximately 25 kD and pI between 7 and 10. These proteins are probably mainly oleosins (Huang, 1996; Kim et al., 2002) and different seed-storage proteins because they are very abundant at the beginning of the germination process and then decline as the endosperm is degraded (Shewry et al., 1995). To satisfy our curiosity about these proteins, we sequenced peptides from three spots that were abundant 2 d after germination, but almost gone after 6 d (Fig. 2). Two of the identified proteins were seed storage proteins, whereas the third

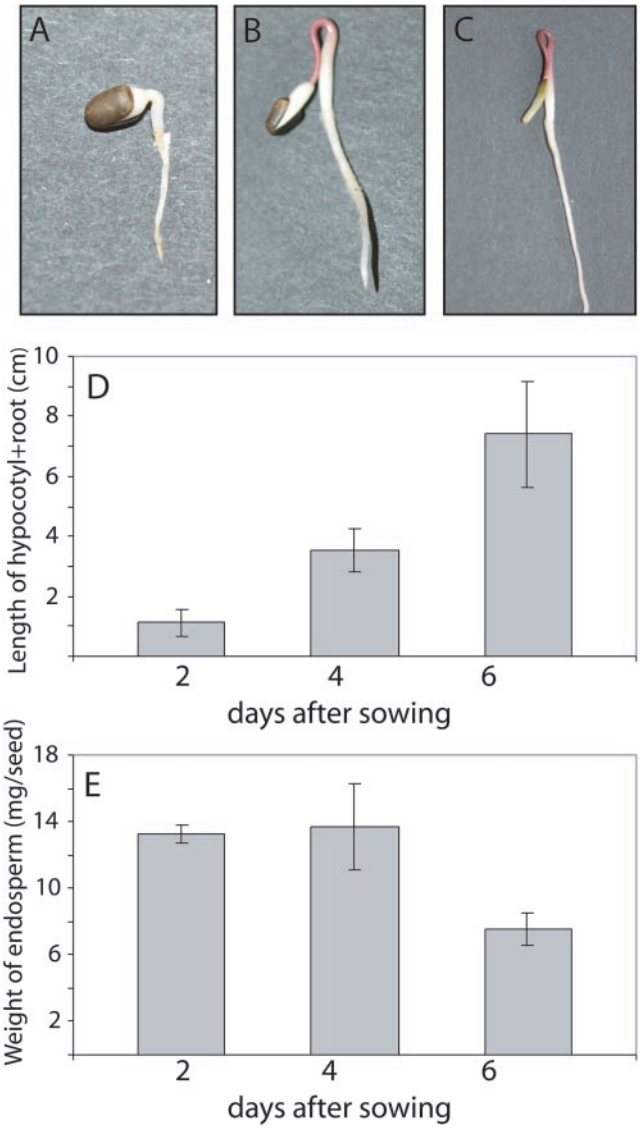

Figure 1. Growth of *E. lagascae* seedlings. A, Seedling 2 d after sowing. B, Seedling 4 d after sowing. C, Seedling 6 d after sowing. D, Graph showing the length (cm) of the hypocotyl + root at 2, 4, and 6 d after sowing. E, The average weight (mg seed^{-1}) of the endosperm in each seed. Values are the means of at least 11 independent measurements. Error bars indicate 1 SD.

spot corresponded to a protein related to an embryo-specific protein from rice (Table I).

In the two-dimensional gels, we identified 17 spots, which increased in size and density during germination (Fig. 2). We cut these spots, indicated in Figure 2, B, C, and F, from the gels, digested the proteins with trypsin, extracted the peptides, and finally sequenced the peptides using a mass spectrometer equipped with an electrospray ion source. The proteins from these spots were mainly involved in basic metabolism like glycolysis (enolase and triosephosphate isomerase), gluconeogenesis (phospho*enol*pyruvate carboxykinase), citric acid cycle (cytosolic malate dehydrogenase), electron transport-chain (mitochondrial malate dehydrogenase), and β-oxidation (glyoxysomal β-ketoacyl-thiolase). We also identified one chaperone, two seed storage proteins, one protein similar to an unknown protein from Arabidopsis, and one protein without significant similarities to any protein in the public databases (Table I).

Some of the more obvious increases in spot size and density could be seen in the lower right corner of the 15% (w/v) gels. Here, in the region of pI from 8 to 10 and molecular mass of around 10 kD, several spots appeared clearly first after 4 d of germination, and they also increased to d 6. Analysis of four spots from this region (Fig. 3) resulted in the discovery of three different LTPs, two of them being the previously characterized ElLTP1 and ElLTP2 (Edqvist and Farbos, 2002). In fact, two of the spots corresponded to ElLTP2, suggesting different isoforms or posttranslational modifications (Table I). From spot 3, a total of five different peptides were sequenced. All of these peptides showed high similarity to ElLTP1 and ElLTP2 as well as LTPs from other organisms. This novel LTP, ElLTP3, also contains the pattern with Cys residues that is characteristic for LTPs (Fig. 4).

Northern-Blot Analysis of ElLTP1 and ElLTP2 mRNAs

Previously, we found ElLTP1 and ElLTP2 transcripts mainly in a fraction from germinating seeds containing cotyledons and endosperm (Edqvist and Farbos, 2002). To get a more detailed understanding of the transcriptional regulation of ElLTP1 and ElLTP2, we separated the endosperm from the cotyledons and isolated total RNA from both tissues. We also analyzed RNA from young flowers and from immature seed pods, to obtain a complementary analysis to the data presented in Edqvist and Farbos (2002), where a northern hybridization was performed with RNA from stems, roots, and leaves from adult plants as well as whole germinating seeds. Both ElLTP1 and ElLTP2 transcripts are very abundant in the endosperm after 4 d of seed germination, but completely missing or below the detection level in the adult flower and seed pod (Fig. 5). In the cotyledons of 4-d-old seedlings, the ElLTP1 transcript was expressed in a significant amount, whereas the transcript of ElLTP2 was not detected at all, indicating a difference in expression patterns between ElLTP1 and ElLTP2. To verify that approximately the same amounts of RNA had been loaded in each well, the membrane was stripped from radioactivity and rehybridized using a probe specific for *E. lagascae* elongation factor 1-α (Fig. 5, top panel).

Western-Blot Analysis of ElLTP1 and ElLTP2

Seedlings were collected 1.5, 2.5, 4, 6, and 7 d after sowing (Fig. 6, top panel). The endosperm was separated from the cotyledons, and proteins were extracted from both tissues. Proteins were also ex-

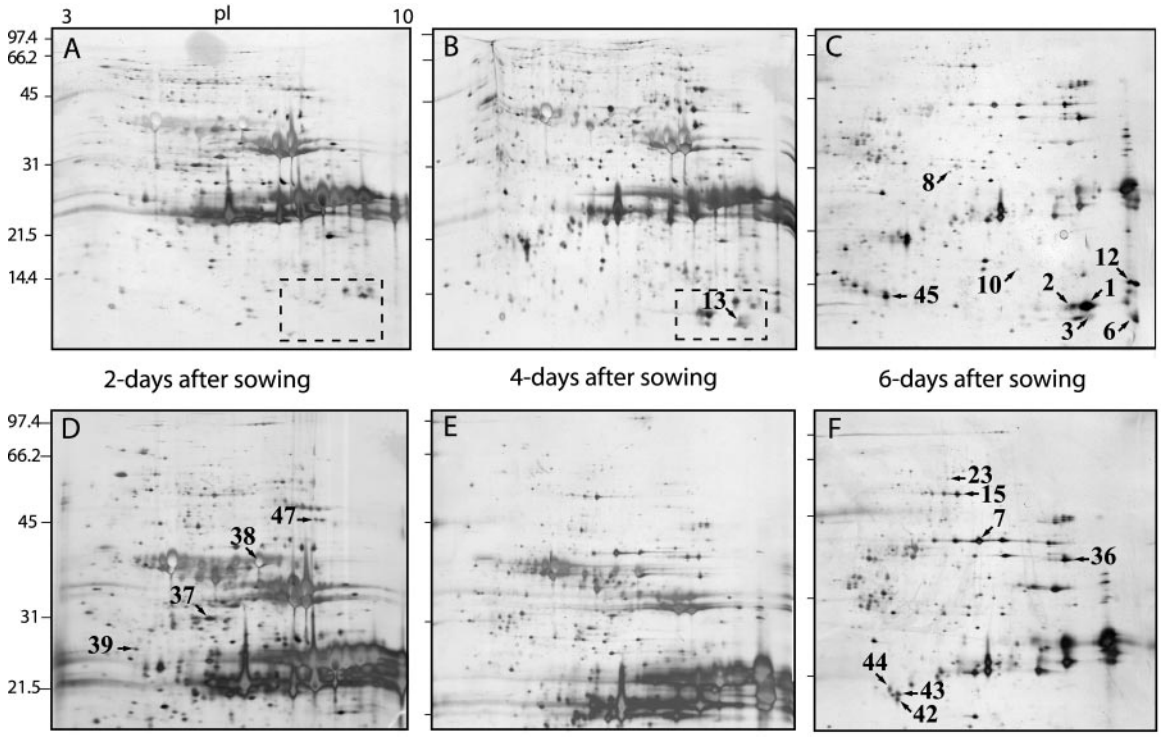

Figure 2. Silver-stained two-dimensional gels that indicate the differences in the endosperm proteome during different stages of seed germination. Proteins were extracted from *E. lagascae* endosperm 2, 4, and 6 d after sowing. Gels containing 15% or 12.5% (w/v) polyacrylamide were used for second dimension electrophoresis. A, 2 d after sowing, 15% (w/v) polyacrylamide. B, 4 d after sowing, 15% (w/v) acrylamide. C, 6 d after sowing, 15% (w/v) polyacrylamide. D, 2 d after sowing, 12.5% (w/v) polyacrylamide. E, 4 d after sowing, 12.5% (w/v) polyacrylamide. F, 6 d after sowing, 12.5% (w/v) polyacrylamide. All six gels were made with the same low molecular mass protein standard having a range from approximately 97 to 14 kD. pI values indicated in gel A, ranging from 3 to 10, apply to all gels. The numbers refer to the protein spot numbers in Table I. Dashed squares in A and B indicate part of gels enhanced in Figure 3.

tracted from adult plant tissues, such as leaves, stems, and roots. The amounts of both ElLTP1 and ElLTP2 are increasing in the endosperm during seed germination. The increase is most evident for ElLTP2 (Fig. 6, bottom panel). In the cotyledons, ElLTP1 protein shows a pattern resembling that of the endosperm, thus the amounts are increasing from d 1.5 to d 7. In the light of the negative results from the northern blots, we were surprised to obtain a positive signal with the anti-ElLTP2 antibodies in the cotyledons. The anti-ElLTP2 signal has a peak in cotyledon abundance at d 4, with very low amounts at d 1.5 and 7. We did detect neither ElLTP1 nor ElLTP2 in the tissue samples from adult plants.

Immunohistochemistry of ElLTP1 and ElLTP2

Immunohistochemistry of ElLTPs in endosperm and cotyledon was performed on seedlings from 4 d after sowing. Staining with the anti-ElLTP1 antibodies is mainly localized to the vascular tissues, more specifically the vessel elements, of the cotyledons (Fig. 7, A and C), but also to the apoplastic space in the endosperm (Fig. 7B). Furthermore, distinct anti-ElLTP1 staining is observed in the region of the endosperm that is closest to the cotyledons. This region consists mainly of collapsed cells (Fig. 7A). There is a gradient of the ElLTP2 protein seen across the endosperm (Fig. 7D), with the stronger signal detected in the inner region of the endosperm close to cotyledons. This is not the case for ElLTP1, which is equally distributed in the endosperm (Fig. 7A). An overview of the ElLTP2 gradient in the endosperm is shown in Figure 7E. The outer region of the endosperm with minimal ElLTP2 abundance is shown in Figure 7F, whereas the inner region of the endosperm with high levels of ElLTP2 protein is shown in Figure 7G. The accumulation of ElLTP2 in the collapsed cell region is shown in Figure 7H. An interesting observation is that the ElLTP2 protein seems to be present inside endosperm cells located close to the collapsed cell region (Fig. 7I). We did not detect any ElLTP2 in the vessel elements in the cotyledons (Fig. 7J).

Detection of PCD by Terminal Deoxynucleotidyltransferase-Mediated dUTP Nick End Labeling (TUNEL) Analysis

It is known that after depletion of the storage material, the endosperm cells undergo senescence by

Table I. *Identified endosperm proteins from E. lagascae*

Spot[a]	Expression[b]	Identity[c]	Score[d]	Molecular Mass[e]	pI[e]	Species	Accession No.
				kD			
1	+	Lipid transfer protein 2	339	9.6	8.2	*E. lagascae*	AAM00273
2	+	Lipid transfer protein 2	276	9.6	8.2	*E. lagascae*	AAM00273
3	+	Lipid transfer protein A	276	9.3	8.7	Castor bean	P10973
6	+	Lipid transfer protein 1	336	9.3	9.2	*E. lagascae*	AAM00272
7	+	Cytoplasmic malate dehydrogenase	461	35.6	6.4	Alfalfa (*Medicago sativa*)	AAB99756
8	+	Triosephosphate isomerase	533	27.1	5.5	Petunia (*Petunia hybrida*)	CAA58230
10	+	Chaperone 10-like protein	195	26.8	7.8	Cotton (*Gossypium hirsutum*)	AAM77651
12	+	Unknown protein	124	13.6	9.2	Arabidopsis	AAM65457
13	+	Lipid transfer protein 1	256	9.3	9.2	*E. lagascae*	AAM00272
15	+	Enolase	487	47.8	5.5	Rubber tree (*Hevea brasiliensis*)	CAC00532
23	+	Phospho*enol*pyruvate dehydrogenase	135	74.4	6.1	Cucumber (*Cucumis sativus*)	AAM00814
36	+	Mitochondrial malate dehydrogenase	137	36.5	8.7	*E. gunnii*	CAA55383
37	−	Embryo-specific protein	133	26.4	5.6	Rice	AAD02495
38	−	Legumin B	392	58.8	8.2	Cotton	AAD09844
39	−	Legumin B	226	58.8	8.2	Cotton	AAD09844
42	+	Unidentified					
43	+	*S*-Adenosylmethionine: 2-demethylmenaquinone methyltransferase	232	17.6	5.3	Arabidopsis	BAB09117
44	+	Legumine-like protein	74	51.9	8.4	*A. europaeum*	CAA64761
45	+	Globulin	98	53.7	8.6	*M. salcifolia*	CAA57847
47	+	Glyoxysomal β-ketoacyl-thiolase	187	48.7	8.5	Canola (*Brassica napus*)	CAA63598

[a] The number refer to the numbers given in Figures 2 and 3. [b] Only protein spots with a time-dependent variation were analyzed. Spots that accumulated by time are denoted +, whereas − indicates that the spot is decreasing during germination. [c] Identifications are based on the results from submitting the obtained peptide sequences to MS BLAST. [d] The scores are the MS BLAST score obtained from submitting the obtained peptide sequences to MS BLAST. [e] The molecular mass and pI values are the theoretical values of the most similar protein.

PCD (Schmid et al., 1999). PCD is also required for differentiation of tracheary elements (Fukuda, 1997). The spatial and temporal localization of ElLTP1 or ElLTP2 to vessels and endosperm indicated that the proteins might be expressed in relation to PCD. To learn more about the progress of PCD in germinating *E. lagascae* seeds, we used the TUNEL assay (Groover and Jones, 1999; Takahashi et al., 1999; Giuliani et al., 2002) on fixed seedlings collected 4 d after sowing (Fig. 8, A, C, and E). The assay involves end-labeling of DNA fragments by using terminal deoxynucleotidyl transferase with dUTP conjugated to a fluorochrome. We obtained TUNEL-positive signals, as shown by the red fluorescence in spots indicated by an arrow in Figure 8A, in the outer regions of the endosperm of the *E. lagascae* seedlings. It is known that the autofluorescence from plant tissues in some cases may be confused with the positive signal from the DNA fragments in the nuclei. To verify that the TUNEL-positive signals were from nuclei, we counter stained the nuclei with 4′,6-diaminophenylindole (DAPI). As shown in Figure 8B, the spots visualized in the TUNEL assay were also fluorescent after staining with DAPI. Thus, our results suggest that in the seedlings collected 4 d after sowing the cells in the outer regions of the endosperm are going through PCD. There were no TUNEL-positive cells in the cotyledons or in the collapsed cell region between endosperm and cotyledons. Seemingly, there are more cells with nuclei in the outer region of the endosperm, compared with the region more close to the cotyledons. No nuclei were detected in the collapsed cell region.

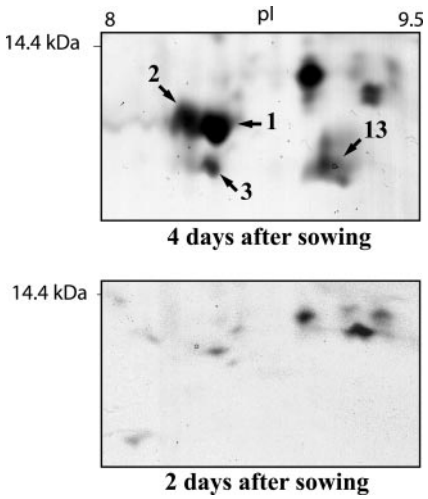

Figure 3. Close-up of the lower right part (indicated in Fig. 2, A and B, by a dashed square) of the 2- and 4-d gels, showing the identified LTP spots in greater detail. The numbers refer to the spot numbers in Table I. The position of the 14.4-kD molecular mass marker as well as approximate pI values of 8 to 9.5 are displayed.

To obtain a positive control of the assay, we also performed TUNEL assays and DAPI counterstaining

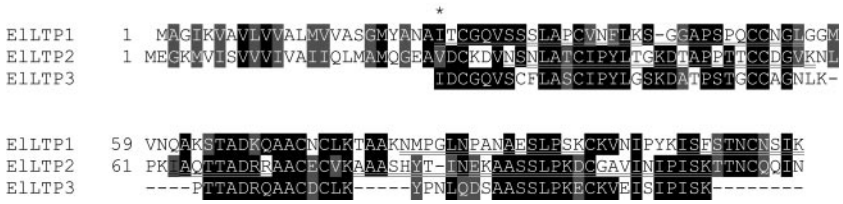

Figure 4. Multiple sequence alignment of ElLTP1 and ElLTP2 with MS/MS acquired peptides of the putative ElLTP3. Black boxes indicate that identical amino acids are present in at least two-thirds of the sequences compared, whereas gray boxes indicate that amino acids with similar physiochemical properties are present in two-thirds of the compared sequences. Peptides sequenced obtained in MS/MS analysis of ElLTP1 and ElLTP2 are underlined. The presumptive N terminus of the mature ElLTP1 is indicated by an asterisk. It should be noted that when sequencing with MS/MS, it is not possible to tell the difference between residues of equal molecular mass, like Leu (L) and Ile (I) or Phe (F) and oxidated Met (M). ElLTP1 and ElLTP2 have the accession numbers AAM00272 and AAM00273 in the National Center for Biotechnology Information database.

on slides treated with DNase I (Fig. 8, C and D). TUNEL assays done without terminal deoxynucleotidyl transferase served as the negative controls of the experiments (Fig. 8, E and F). It is generally accepted that a positive TUNEL assay is an insufficient criterion for defining PCD because TUNEL positive nuclei can be formed by nonspecific chromosome breakage (Collins et al., 1992; Jones and Dangl, 1996). However, based on studies in castor bean (Schmid et al., 1999), we can presume that our positive results are characteristics of a somewhat ordered process of chromatin degradation, in which the DNA has been broken down by an endonuclease.

DISCUSSION

Here, we have shown that ElLTP1 and ElLTP2 are accumulating in the endosperm as the endosperm cells undergo senescence by PCD. In endosperm of 4-d-old seedlings, ElLTP2 is mainly localized to inner regions of the endosperm. The TUNEL assay and DAPI staining showed that at this time point PCD had progressed to the outer regions of the en-

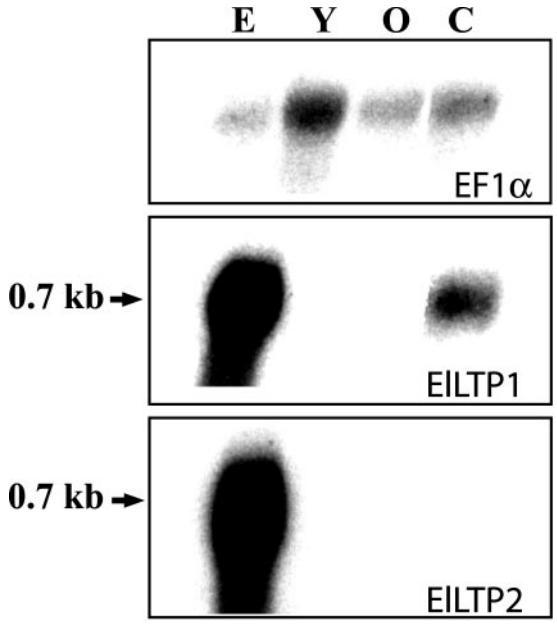

Figure 5. Northern-blot analysis of RNA isolated from *E. lagascae*. RNA was isolated from endosperm (E) and cotyledons (C) of germinating seeds 4 d after sowing and from the flowers (stamens and carpels) of adult plants. Old (O) and young (Y) indicates stages in flower development were Y is a bud and O an immature seed pod. The top panel shows hybridization to a probe specific for *E. lagascae* elongation factor 1-α (EF1α), to verify that roughly the same amounts of RNA had been loaded in each well. The middle panel displays hybridization to the *ElLTP1* probe, and the bottom panel displays hybridization to the *ElLTP2* probe. The numbers to the left indicates approximate transcript sizes.

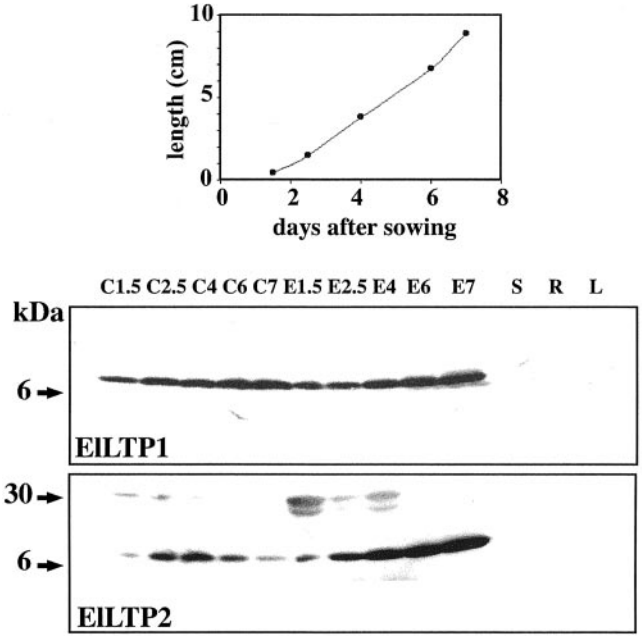

Figure 6. Western-blot analysis of ElLTP1 and ElLTP2. The diagram (top panel) shows average hypocotyl lengths of the seedlings used in the western-blot experiment. Total proteins were extracted from cotyledons (C) and endosperm (E) collected from seedlings at 1.5, 2.5, 4, 6, and 7 d after sowing. Stems (S), roots (R), and leaves (L) were from adult plants. Protein detection was performed using affinity-purified anti-ElLTP1 (middle panel) or anti-ElLTP2 (bottom panel) antisera. Approximate protein sizes according to the protein standard are indicated to the left.

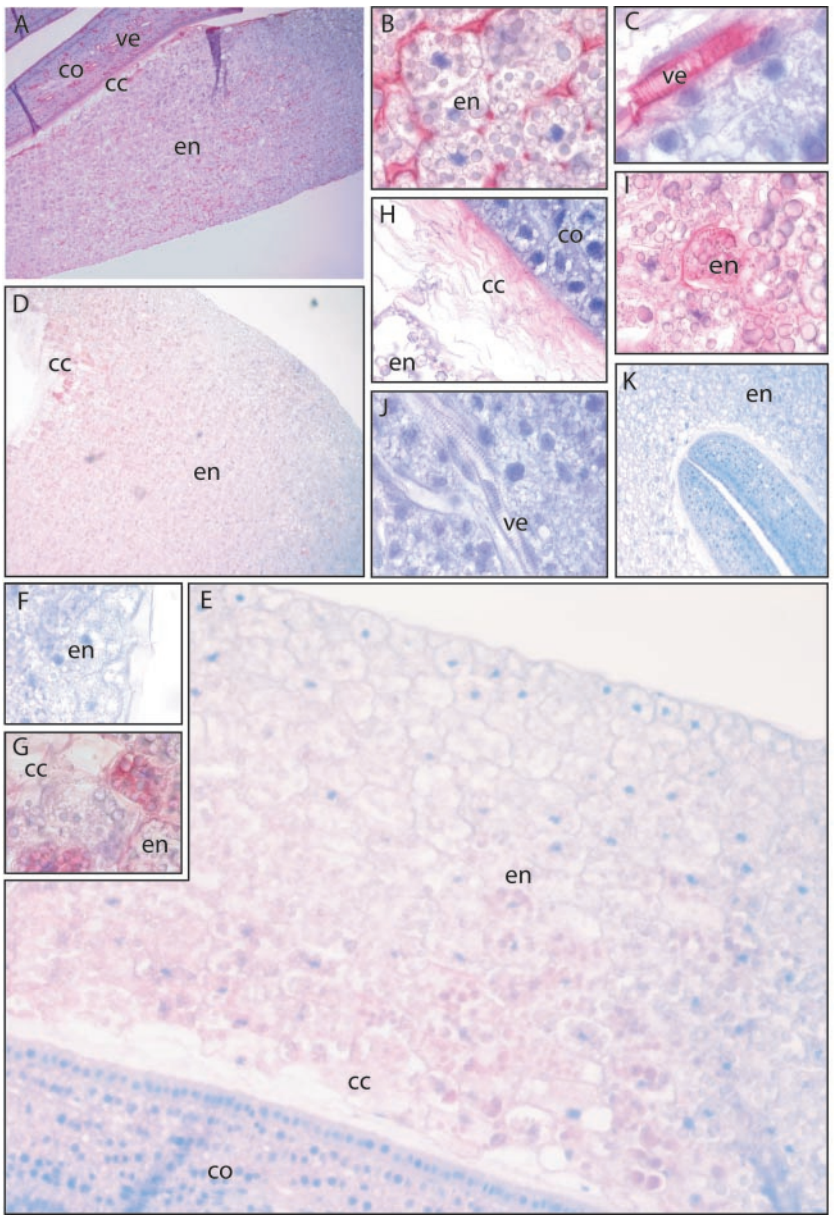

Figure 7. Immunohistochemistry using antibodies against ElLTP1 and ElLTP2 on sectioned seedlings collected 4 d after sowing. Red color indicates detection of antigen, and blue color is counter staining of nuclei with Mayers hematoxylin. A through C, Result after staining with the anti-ElLTP1 antibody. D through J, Result with the anti-ElLTP2 antibody. K, Negative control, which is stained without primary antibody. A, Overview of anti-ElLTP1 staining in the endosperm (en), collapsed cell region (cc), and cotyledons (co). B, Detection of the ElLTP1 in apoplastic space in the middle part of the endosperm. C, Detection of ElLTP1 in the vessel elements (ve) of the cotyledons. D, Overview of anti-ElLTP2 staining in the endosperm and collapsed cell region. E, A closer view of the detection of ElLTP2 in endosperm, cc region and the cotyledons. F, The weak anti-ElLTP2 staining in the outmost part of the endosperm. G, A strong anti-ElLTP2 signal was obtained from the inner part of the endosperm. H, Detection of ElLTP2 in the cc region. I, In the endosperm, ElLTP2 was detected between and also inside cells. J, ElLTP2 was not detected in vessel elements or other cells of the cotyledons.

dosperm. Thus, it seems that ElLTP2 is most abundant in dying tissues. Lipids and fatty acids are major building blocks for cell membranes and for the cuticular waxes. The expanding cotyledons need a sufficient supply of such building blocks to ensure proper growth and development. Many complex lipid structures of the dead cells, such as parts of cellular and organellar membranes, are probably turned over and re-used in the growing parts of the plant. This implies that there must be an active transport of lipids from the dead endosperm cells to the growing cotyledons. The ElLTP2 gradient in the endosperm may indicate a movement of ElLTP2, and perhaps also lipids, from the endosperm to the epicuticulary cell layer where the lipids are absorbed by the growing cotyledons. Interestingly, we detected anti-ElLTP2 signals in protein extracts isolated from the cotyledons, even though we did not detect any ElLTP2 transcripts there. In this context, we suggest that ElLTP2 function as a apoplastic carrier when lipid components from the senescent cells of the endosperm are relocalized to the growing cotyledons. A reasonable hypothesis is that the lipids transferred by ElLTP2 are used in epidermal growth and development.

It has previously been shown that during PCD of plant cells, proteases are released from dying cells and may damage and cause necrosis of neighboring cells (Beers and Freeman, 1997; Kuriyama and Fukuda, 2002). Plant cells may have a regulated mechanism to protect its cells from autolytic enzymes released from dying or dead cells. The nature of such a mechanism that limit the damage caused by autolytic enzymes is not known. However, a putative LTP

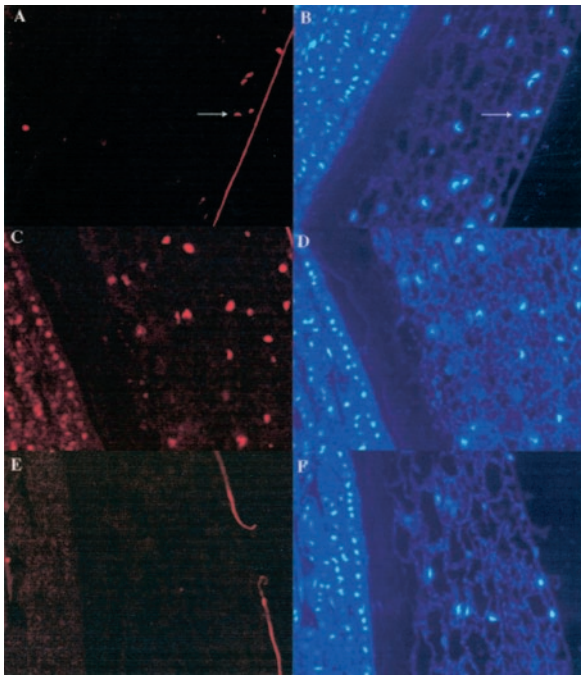

Figure 8. nDNA fragmentation in germinating *E. lagascae* seedlings. The progress of PCD was analyzed using the TUNEL-assay that detects DNA-fragmentation. Sections were prepared from endosperm and cotyledons from seedling collected 4 d after sowing. A, DNA-fragmentation was detected in the outermost layers of the endosperm. The arrows point toward TUNEL-positive nuclei. B, The section from A was counter stained with DAPI to visualize the nuclei. The arrows in A and B point toward the same nucleus after detection of the red fluorochrome from the TUNEL assay (A) or after detection of the DAPI staining (B). C, The positive control slides were treated with DNase I. D, DAPI staining of the positive control slide. E, In the negative control of the TUNEL assay, terminal deoxynucleotidyl-transferase was omitted from the experiment. F, Results from counter staining of the negative control slide with DAPI.

called TED4, which is specifically expressed in cells differentiating into tracheary elements in zinnia (*Zinnia elegans*) cultures, forms a complex with a proteasome and thereby inhibits proteasome activity (Endo et al., 2001). LTPs have also been shown to inhibit protease activities in green malt (Jones and Marinac, 1997). Here, we have shown that ElLTP1 is present in the vessel elements in the developing cotyledons. We suggest that this may indicate that ElLTP1, like TED4, is functioning as a protease inhibitor during the differentiation of tracheary elements. ElLTP1 is also present in the apoplastic space of the endosperm and in the collapsed cell region between the endosperm and cotyledons. This localization pattern could indicate a function as a protease inhibitor forming a protective barrier. This barrier would then prevent the cells from necrosis as nearby endosperm cells are going through PCD, releasing destructive proteases to the surrounding environment. However, it is also possible that ElLTP1, like we have suggested for ElLTP2, is involved in transferring lipids from dead cells to growing tissues.

In the silver-stained two-dimensional gels, several spots were shown to correspond to ElLTP1 and ElLTP2. Moreover, to the left of the ElLTP3 spot there is a very weak neighboring spot (Fig. 4) that we speculate also correspond to ElLTP3. These complicated patterns indicate that there are multiple isoforms or that posttranslational modifications are present in the LTPs. The pattern of the tandem ElLTP2 spots resembles that of a phosphorylation where the modified, and thus more acidic protein have a higher M_r. The tandem mass spectrometry (MS/MS) sequence data have not supplied any further information on the reason for the change of pI and mass. So, to obtain a better view of possible phosphorylation sites in the LTPs of this study, ElLTP1 and ElLTP2 sequences were submitted to the NetPhos 2.0 prediction server at the Centre for Biological Sequence Analysis (Blom et al., 1999; http://www.cbs.dtu.dk/services/NetPhos/). NetPhos evaluates all Ser, Thr, and Tyr residues in their context, and reports a score for phosphorylation possibility. According to the NetPhos server ElLTP1 has a possible phosphorylated Ser residue at position 45 and ElLTP2 has a candidate in the Thr at position 22. The NetPhos scores for these two positions are 0.948, for the ElLTP1 Ser, and 0.979 for the ElLTP2 Thr. These scores are both high above the threshold, close to the maximum score of 1.0, suggesting that both ElLTP1 and ElLTP2 may contain phosphorylated residues. It was previously shown that four wheat LTPs were substrates for a calcium-dependent protein kinase purified from wheat germ (Neumann et al., 1994). Moreover, a lipid-like modification was recently discovered in barley LTP1 (Lindorff-Larsen et al., 2001). The biological relevance for posttranslational modifications of LTPs remains to be analyzed.

Together, these results indicate that the work initiated here is important for the future investigations into the recycling and degradation of cell components during senescence. It will be of high interest to investigate in further detail the function of LTPs during PCD. Future research will include an analysis of the expression of LTPs during PCD in other tissues than endosperm, but we will also search for interacting partners to the ElLTPs. Also, a more detailed investigation of the role of the probable posttranslational modifications could prove productive. Further, the creation of loss-of-function mutants in Arabidopsis could illuminate the physiological role of the LTPs.

MATERIALS AND METHODS

Plant Material

Euphorbia lagascae Spreng. seeds were soaked with tap water for approximately 4 h and then grown in moist vermiculite in a greenhouse facility during one to 7 d. Other seeds were cultivated in soil to adult plants. Tissues were stored at −80°C, for shorter periods of time, until used. The *E. lagascae* seeds were a kind gift from Prof. Sten Stymne (Department of Crop Science, SLU, Alnarp, Sweden).

Preparation of Protein Extracts for Two-Dimensional Gel Electrophoresis

Total protein extracts were prepared from the endosperm of 2-, 4-, and 6-d seedlings. After disruption of the endosperm cells, using a mortar and pestle in liquid nitrogen, total protein was extracted by a trichloroacetic acid (TCA) method described by Tsugita and Kamo (1999). Frozen plant tissue powder (0.1–0.2 g) was suspended in 5 mL of TCA solution (20 mM dithiothreitol [DTT; Amersham Biosciences, Uppsala] and 10% [w/v] TCA [Merck, Darmstadt, Germany] in acetone). After 45 min at −20°C, the suspension was centrifuged at 35,000*g* for 15 min at 4°C. The precipitate was resuspended in 5 mL of wash solution (20 mM DTT and 2 mM EDTA [Merck] in acetone) and placed at −20°C for 1 h. This suspension was centrifuged (35,000*g*, 15 min, and 4°C), and the pellet was again resuspended in wash solution immediately followed by another centrifugation. After centrifugation, the precipitate was lyophilized until absolutely dry. All of the precipitate was suspended in 0.5 mL of electrofocusing buffer (8 M urea, 2% [w/v] CHAPS, and traces of bromphenol blue) and heavily stirred at room temperature for several hours followed by centrifugation at 19,000*g* for 10 min. The supernatant was removed and stored in −20°C until used in two-dimensional gel electrophoresis.

First and Second Dimension Gel Electrophoresis

An appropriate amount of TCA-precipitated proteins were diluted with fresh electrofocusing buffer to obtain 20 mg of TCA precipitate in 350 μL of buffer. To these 350 μL, DTT and IPG buffer (Amersham Biosciences AB) were added to concentrations of 20 mM and 0.5%, respectively. The protein solutions were loaded on to dry polyacrylamide gel strips with immobilized pH gradients of 3 to 10 (Immobiline Dry Strip, pH 3–10 NL, 18 cm, Amersham Biosciences AB) put in IPGphor strip holders placed on an IPGphor Isoelectric Focusing System (Amersham Biosciences AB). Gels were then rehydrated for 10 min, and isoelectric focusing was done according to the following scheme: 50 V for 12 h, 500 V for 1 h, 1,000 V for 1 h, and finally 8,000 V for 36,000 volthours up to a total of 38,101 volthours. Equilibration of gel strips was performed in an SDS equilibration buffer (50 mM Tris-Cl, pH 8.8, 6 M urea, 30% [w/v] glycerol, 2% [w/v] SDS, and bromphenol blue) with DTT (10 mg mL^{-1}) for 15 min and then with iodoacetamide (25 mg mL^{-1}) for 15 min. Second dimension gel electrophoresis was performed on 15% and 12.5% (w/v) polyacrylamide gels (0.4 M Tris, pH 8.8, and 1% [w/v] SDS) with a low M_r protein standard (SDS-PAGE Molecular Weight Standards, Bio-Rad Laboratories, Hercules, CA) used according to manufacturer's instructions, using a 0.1% (w/v) SDS running buffer (25 mM Tris, 192 mM Gly, and 0.1% [w/v]SDS).

Silver Staining and Analysis of Two-Dimensional Gels

Gels were stained with silver nitrate essentially according to a protocol by Shevchenko et al. (1996). The gels were fixed by immersing them into a fix solution (methanol:acetic acid:water at 45:5:45) overnight. The acid was then removed by rinsing the gels for 1 to 2 h in water. To increase the sensitivity of the staining, the gels were incubated for 1 min in 0.8 mM sodium thiosulphate. After washing with water, gels were bathed in a 6 mM silver nitrate solution for 20 min at 4°C in darkness. Residual silver ions were removed with two washes of water. Reduction of protein-bound silver ions was performed using a development solution (0.015% [v/v] formaldehyde and 0.25 M sodium carbonate) until a sufficient level of staining had been reached. The development solution was replaced with a fresh portion when the first one turned brownish. Development was quenched using 1% (v/v) acetic acid, and the gels were then stored at 4°C for several months in the acid. For longer storage, the gels were dried in a Drygel Sr. (Hoefer, San Francisco). Silver-stained gels were scanned using a scanner (GS-710 Calibrated Imaging Densitometer, Bio-Rad Laboratories) equipped with PDQuest Two-Dimensional Gel Analysis Software (Bio-Rad Laboratories).

In Gel Digestion and Gel Extraction of Peptides

A slightly modified version of a method described by Wilm et al. (1996) was used. Protein spots of interest were excised using a sharp knife, cut into smaller parts, and then washed in water. To dry the gel pieces, 100 μL of acetonitrile was added to each tube followed by shaking for 15 min at room temperature, removal of liquid, and then vacuum centrifugation for 15 min. Gel pieces were rehydrated in 20 μL of digestion buffer (100 mM sodium bicarbonate, 5 mM calcium chloride, and 25 ng μL^{-1} trypsine [Invitrogen, Carlsbad, CA]) at 4°C for 1 h. Excess liquid was removed, and another 20 μL of digestion buffer, without trypsine, was added. Reactions were incubated in 37°C overnight. The supernatant was collected, and gel pieces were incubated in 50 μL of 25 mM sodium bicarbonate for 15 min with shaking at 37°C, this was followed by removal of liquid from the gel with 50 μL of acetonitrile as previously described. Fifty microliters of 5% (v/v) formic acid was added, and the gel pieces were incubated as above. The gel pieces were again dried with acetonitrile and stored at −20°C. All supernatants from the same gel pieces were collected and pooled. The liquid was evaporated in a vacuum centrifuge, and the pellets were stored at −20°C.

Peptide Analysis by Mass Spectrometry

Peptide pellets were resuspended in 1 μL of 80% (v/v) formic acid and then quickly diluted to an 8% (v/v) solution by adding 10 μL of water. Peptide solutions were sonicated for 5 min before loading 5 μL of it to a nanoelectrospray glass capillary (Protana Engineering A/S, Odense, Denmark) with an R2 resin (POROS 20 R2, Applied Biosystems, Foster City, CA), binding proteins by hydrophobic interactions. R2 capillaries were prepared by loading 1.5 μL of R2 suspension, giving approximately 300 to 400 nL of resin, to the capillary. Excess fluid was removed by centrifugation. The resin was washed twice with 5 μL of 0.5% (v/v) formic acid. After the wash solution had been centrifuged through the capillary the peptide sample was added followed by two washes with 5 μL of 0.5% (v/v) formic acid. Peptides were eluted, by adding 0.5 μL of 25% (v/v) acetonitrile in 0.5% (w/v) formic acid and then 0.5 μL of 50% (v/v) acetonitrile in 0.5% (w/v) formic acid followed by centrifugation, into Au/Pd-coated nanoelectrospray glass capillaries (Protana Engineering A/S). This method is a modified version of that described by Wilm et al. (1996). To acquire peptide sequence data, capillaries were inserted into a quadropole time-of-flight mass spectrometry instrument (Micromass Q-Tof, Micromass Ltd., Manchester, UK) with a nanospray ion source. The capillary voltage was set to 800 to 900 V, and the cone voltage to 40 V. Argon was used as collision gas and the kinetic energy was set to between 20 and 40 eV. Peptide sequence data was analyzed using the BioLynx program of the MassLynx NT software package (v3.4, Micromass Ltd.).

Bioinformatics

Peptide sequences obtained by MassLynx were subjected to BLAST using blastp (Altschul et al., 1997) at the National Center for Biotechnology Information (http://www.ncbi.nlm.nih.gov/BLAST/) and MS BLAST (Shevchenko et al., 2001) at the European Molecular Biology Laboratory (http://dove.embl-heidelberg.de/Blast2/msblast.html). Multiple sequence alignment was created using ClustalX (Thompson et al., 1997), and the resulting similarities were then visualized by subjecting the alignment to Boxshade (K. Hofmann and M. Baron, unpublished data).

RNA Isolation and Northern Hybridization

E. lagascae total RNA was isolated from the endosperm and cotyledons of 4-d-old seedlings and from young flowers and seed pods from adult plants. Isolation was performed using a guanidine hydrochloride method previously described by Logemann et al. (1987). For northern-blot analysis, 10 μg of total RNA from each sample was dissolved in sample buffer (20 mM MOPS, 1 mM EDTA, 5 mM sodium acetate, 50% [v/v] formamide, and 2.2 M formaldehyde, pH 7.9) and separated by electrophoresis on an agarose gel (1.2% [w/v] agarose, 3% [v/v] formaldehyde, 20 mM MOPS, 1 mM EDTA, and 5 mM sodium acetate). The RNA was transferred onto a nylon membrane (HybondN+, Amersham Biosciences) and fixed to the membrane by UV-cross-linking (UVC 500, Hoefer) according to the manufacturer's instructions. Immobilized RNA was hybridized with gene-specific probes from the ElLTP1 and ElLTP2 genes (Edqvist and Farbos, 2002) and with an *E. lagascae* elongation factor 1-α (EF1-α) probe. Labeled membranes were then subjected to autoradiography. Before reprobing, radioactivity was stripped from the membrane by immersing it into boiling 0.5% (w/v) SDS for a few minutes until no radioactivity could be detected. Stripping was verified by autoradiography.

Preparation of Antibodies against ElLTP1 and ElLTP2

On the basis of the three-dimensional structures of maize (*Zea mays*) and rice (*Oryza sativa*) LTPs (Lee et al., 1998), the L3 loop and parts of H4 helix were chosen as an appropriate target due to its exposed position. Synthetic peptides were created based on the amino acid sequences of this region with the addition of a Cys residue in the N-terminal for coupling to bovine serum albumin (BSA). The BSA-coupled peptides had the following sequences: ElLTP1 CKNMPGLNPAN and ElLTP2 CASHYTINEKA. AgriSera (Vännäs, Sweden) performed peptide synthesis, coupling to BSA, immunization of rabbits, bleedings, serum preparations, and affinity purifications of the ElLTP1 and ElLTP2 antibodies. The procedures are described by Bergman et al. (2000).

Protein Extraction and Western Blotting

Total protein extracts were prepared from endosperm and cotyledon from seedlings collected 1.5, 2.5, 4, 6, and 7 d after sowing. Additionally, protein extracts from stems, leaves, and roots were generated from adult plants. Ten milligrams of each tissue sample was grinded in 100 μL of 2× SDS sample buffer (125 mM Tris-HCl, pH 6.8, 4% [v/v] SDS, 20% [v/v] glycerol, 0.01% [w/v] bromphenol blue, and 20 mM DTT) and then diluted with 100 μL of phosphate-buffered saline (PBS; 80 mM disodium hydrogen phosphate, 20 mM sodium dihydrogen phosphate, and 100 mM sodium chloride) at pH 7.4. Before loading on a gel, the sample was heated to 90°C for 5 min and then centrifuged. Five microliters, corresponding to 250 μg of fresh tissues, from each sample was loaded to the gel as well as a protein standard (MultiMark Multi-Colored Standard, Invitrogen), used according to manufacturer's instructions. Proteins were separated by electrophoresis on 8% to 16% (w/v) SDS-polyacrylamide gels (Novex Pre-Cast Gels, Invitrogen; Laemmli, 1970) using an SDS running buffer (0.1% [w/v] SDS, 25 mM Tris, and 192 mM Gly). Proteins were then transferred to a membrane (Hybond ECL nitrocellulose membrane, Amersham Biosciences) by electroblotting (Towbin et al., 1979) at 400 mA for 2 h at 4°C, as described by the manufacturer, using a protein transfer buffer containing methanol (25 mM Tris, 20 mM Gly, and 20% [v/v] methanol). After transfer, the membranes were removed and used directly in subsequent immunodetection. Nonspecific binding of antibodies to the membranes was blocked by immersing the membranes in 5% (w/v) dry-milk powder in Tris-buffered saline plus Tween 20 (20 mM Tris-HCl and 0.2 M sodium chloride at pH 7.6 with 0.1% [v/v] Tween 20) at 4°C overnight. After washing, the membranes were treated with affinity-purified rabbit antibodies against the synthetic peptides ElLTP1 and ElLTP2. The primary antibodies were diluted 1:1,000. Subsequent detection of primary antibodies was performed using the ECL detection system from Amersham Biosciences. Secondary anti-rabbit antibodies were diluted 1:2,000. All dilutions and washes were in Tris-buffered saline plus Tween 20.

Immunohistochemistry

Four-day-old seedlings were used for all immunohistochemistry experiments. The root and hypocotyl were removed from the seedling with a knife. After that the endosperm with comprised cotyledons were fixed (4% [w/v] paraformaldehyde and 0.25% [w/v] glutaraldehyde in 0.1 M phosphate buffer pH 7.0) for approximately 16 h in room temperature. Subsequently, the seedlings were rinsed in water and then dehydrated in a graded ethanol series from 70% to 99.5%. Ethanol was finally completely removed by soaking the tissue in two changes of xylene for 1 h each before imbedding in Paraplast Plus (Sigma-Aldrich, St. Louis). Sections of 5 μm were cut using a steel blade (Rotary Microtome HM330, Microme, Heidelberg Germany), transferred to a 37°C water bath to smooth down, and then put on 3-aminopropyltriethoxysilane (Sigma-Aldrich)-precoated glass slides. Slides were incubated overnight at 37°C. Sections were deparafinized by washing in xylen for 20 min and then rehydrated in an ethanol series followed by washing in water for 1 min.

For immunohistochemistry, sections were rinsed in PBS at pH 7.4 for 5 min followed by blocking of unspecific binding using PBS with 5% (w/v) dry-milk powder. Subsequent to blocking, primary antibodies from affinity-purified rabbit sera, diluted in PBS with 5% (w/v) dry-milk powder, were distributed to the sections. Detection of primary antibodies was performed using the LSAB detection kit from DAKO (Glostrup, Denmark), according to the manufacturer's instructions. Counterstaining was performed using Mayers hematoxylin (Histolab, Göteborg, Sweden), coloring all nuclei blue, according to instructions. All washes were in PBS at pH 7.4.

In Situ Detection of DNA Fragmentation

DNA fragmentation was detected in 5-μm sections of the same material used for immunocytochemistry, by TUNEL analysis (Gorczyca et al., 1993). This assay was performed essentially according to Filonova et al. (2000) using the In Situ Cell Death Detection Kit, TMR red from Roche Diagnostics (Mannheim, Germany). Permeabilization was performed using Proteinase K (10 μg mL^{-1} in 10 mM TRIS-HCl, pH 7.6), and the positive control was treated with DNase I (Amersham Biosciences) for 10 min to induce DNA fragmentation; negative control was treated omitting terminal deoxynucleotidyltransferase according to the manufacturer's instructions. nDNA was stained with 1 μg mL^{-1} of DAPI (Roche Diagnostics) in PBS for 5 min at room temperature. Slides were then washed with PBS and distilled water, covered by Fluorsave (Calbiochem, San Diego), and examined with a microphot-FXA fluorescence microscope using FICT and UV-2A sets of filters for TUNEL detection and DAPI, respectively.

ACKNOWLEDGMENTS

We gratefully acknowledge the technical support of Ingrid Schenning, Ulla Pihlgren, and Ingrid Eriksson. Dr. Håkan Larsson is recognized for consultation concerning protein extraction and peptide sequence determination. Dr. Lada Filonova and Dr. Peter Bozhkov are acknowledged for helping us with the TUNEL assays. We thank Dr. Kristina Blomqvist for valuable comments on the manuscript.

Received January 27, 2003; returned for revision February 28, 2003; accepted March 10, 2003.

LITERATURE CITED

Altschul SF, Madden TL, Schäffer AA, Zhang J, Zhang Z, Miller W, Lipman DJ (1997) Gapped BLAST and PSI-BLAST: a new generation of protein database search programs. Nucleic Acids Res **25:** 3389–3402

Aubert S, Gout E, Bligny R, Marty-Mazars D, Barrieu F, Alabouvette J, Marty F, Douce R (1996) Ultrastructural and biochemical characterization of autophagy in higher plant cells subjected to carbon deprivation: control by the supply of mitochondria with respiratory substrates. J Cell Biol **133:** 1251–1263

Beers EP, Freeman TB (1997) Proteinase activity during tracheary element differentiation in zinnia mesophyll cultures. Plant Physiol **113:** 873–880

Beevers H (1980) The role of the glyoxylate cycle, *In* PK Stumpf, ed, The Biochemistry of Plants, Vol 4. Academic Press, New York, pp 117–130

Bergman P, Edqvist J, Farbos I, Glimelius K (2000) Male-sterile tobacco displays abnormal mitochondrial *atp*1 transcript accumulation and reduced floral ATP/ADP ratio. Plant Mol Biol **42:** 531–544

Blein JP, Coutos-Thévenot P, Marion D, Ponchet M (2002) From elictins to lipid-transfer proteins: a new insight in cell signalling involved in plant defence mechanisms. Trends Plant Sci **7:** 293–296

Blom N, Gammeltoft S, Brunak S (1999) Sequence- and structure-based prediction of eukaryotic protein phosphorylation sites. J Mol Biol **294:** 1351–1362

Buhot N, Douliez JP, Jacquemard A, Marion D, Tran V, Maume BF, Milat ML, Ponchet M, Mikes V, Kader JC et al. (2001) A lipid transfer protein binds to a receptor involved in the control of plant defence responses. FEBS Lett **509:** 27–30

Cammue BP, Thevissen K, Hendriks M, Eggermont K, Goderis IJ, Proost P, Van Damme J, Osborn RW, Guerbette F, Kader JC (1995) A potent antimicrobial protein from onion seeds showing sequence homology to plant lipid transfer proteins. Plant Physiol **109:** 445–455

Collins RJ, Harmon BV, Gobe GC, Kerr JF (1992) Internucleosomal DNA cleavage should not be the sole criterion for identifying apoptosis. Int J Radiat Biol **61:** 451–453

Doelling JH, Walker JM, Friedman EM, Thompson AR, Vierstra RD (2002) The APG8/12-activating enzyme APG7 is required for proper nutrient recycling and senescence in *Arabidopsis thaliana*. J Biol Chem **277:** 33105–33114

Douliez JP, Jegou S, Pato C, Molle D, Tran V, Marion D (2001) Binding of two mono-acylated lipid monomers by the barley lipid transfer protein, LTP1, as viewed by fluorescence, isothermal titration calorimetry and molecular modelling. Eur J Biochem **268:** 384–388

Douliez JP, Michon T, Elmorjani K, Marion D (2000) Structure, biological and technological functions of lipid transfer proteins and indolines, the major lipid binding proteins from cereal kernels. J Cereal Sci **32:** 1–20

Edqvist J, Farbos I (2002) Characterization of germination-specific lipid transfer proteins from *Euphorbia lagascae*. Planta **215:** 41–50

Edqvist J, Farbos I (2003) A germination-specific epoxide hydrolase from *Euphorbia lagascae*. Planta **216:** 403–412

Endo S, Demura T, Fukuda H (2001) Inhibition of proteasome activity by the TED4 protein in extracellular space: a novel mechanism for protection of living cells from injury caused by dying cells. Plant Cell Physiol **42:** 9–19

Filonova LH, Bozhkov PV, Brukhin VB, Daniel G, Zhivotovsky B, von Arnold S (2000) Two waves of programmed cell death occur during formation and development of somatic embryos in the gymnosperm, Norway spruce. J Cell Sci **113:** 4399–4411

Fukuda H (1997) Tracheary element differentiation. Plant Cell **9:** 1147–1156

Garcia-Olmedo F, Molina A, Segura A, Moreno M (1995) The defensive role of nonspecific lipid-transfer proteins in plants. Trends Microbiol **3:** 72–74

Giuliani C, Consonni G, Gavazzi G, Colombo M, Dolfini S (2002) Programmed cell death during embryogenesis in maize. Ann Bot **90:** 287–292

Gomar J, Petit MC, Sodano P, Sy D, Marion D, Kader JC, Vovelle F, Ptak M (1996) Solution structure and lipid binding of a nonspecific lipid transfer protein extracted from maize seeds. Protein Sci **5:** 565–577

Gorczyca W, Gong J, Darzynkiewicz Z (1993) Detection of DNA strand breaks in individual apoptotic cells by the *in situ* terminal deoxynuleotidyl transferase and nick translation assay. Cancer Res **53:** 1945–1951

Groover A, Jones AM (1999) Tracheary element differentiation uses a novel mechanism coordinating programmed cell death and secondary cell wall synthesis. Plant Physiol **119:** 375–384

Hanaoka H, Noda T, Shirano Y, Kato T, Hayashi H, Shibata D, Tabata S, Ohsumi Y (2002) Leaf senescence and starvation-induced chlorosis are accelerated by the disruption of an Arabidopsis autophagy gene. Plant Physiol **129:** 1181–1193

Heinemann B, Anderon KV, Nielsen PR, Bech LM, Poulsen FM (1996) Structure in solution of a four-helix lipid binding protein. Protein Sci **5:** 13–23

Horvath BM, Bachem CWB, Trindade LM, Oortwijn MEP, Visser RGF (2002) Expression analysis of a family of *nsLTP* genes tissue specifically expressed throughout the plant and during potato tuber life cycle. Plant Physiol **129:** 1494–1506

Huang AH (1996) Oleosins and oil bodies in seeds and other organs. Plant Physiol **110:** 1055–1061

Ichimura Y, Kirisako T, Takao T, Satomi Y, Shimonishi Y, Ishihara N, Mizushima N, Tanida I, Kominami E, Ohsumi M et al. (2000) A ubiquitin-like system mediates protein lipidation. Nature **408:** 488–492

Jones AM, Dangl JL (1996) Logjam at the Styx: programmed cell death in plants. Trends Plant Sci **1:** 114–119

Jones BL, Marinac LA (1997) Purification, identification and partial characterization of a barley protein that inhibits green malt endoproteinases. J Am Soc Brew Chem **55:** 58–64

Kader JC (1996) Lipid-transfer proteins in plants. Annu Rev Plant Physiol Plant Mol Biol **47:** 627–654

Kader JC, Julienne M, Vergnolle C (1984) Purification and characterization of a spinach-leaf protein capable of transferring phospholipids from liposomes to mitochondria or chloroplasts. Eur J Biochem **139:** 411–416

Kim HU, Hsieh K, Ratnayake C, Huang AH (2002) A novel group of oleosins is present inside the pollen of *Arabidopsis*. J Biol Chem **277:** 22677–22684

Kuriyama H, Fukuda H (2002) Developmental programmed cell death in plants. Curr Opin Plant Biol **5:** 568–573

Laemmli UK (1970) Cleavage of structural proteins during the assembly of the head of bacteriophage T4. Nature **227:** 680–685

Lee JY, Min K, Cha H, Shin DH, Hwang KY, Shu SW (1998) Rice nonspecific lipid transfer protein: The 1.6 Å crystal structure in the unliganded state reveals a small hydrophobic cavity. J Mol Biol **276:** 437–448

Lindorff-Larsen K, Lerche MH, Poulsen FM, Roepstorff P, Winther JR (2001) Barley lipid transfer protein, LTP1, contains a new type of lipid-like post-translational modification. J Biol Chem **276:** 33547–33553

Logemann J, Shell J, Willmitzer L (1986) Improved method for the isolation of RNA from plant tissue. Anal Biochem **163:** 16–20

Maldonado AM, Doerner P, Dixon RA, Lamb CJ, Cameron RK (2002) A putative lipid transfer protein involved in systemic resistance signalling in *Arabidopsis*. Nature **2002:** 399–403

Neumann GM, Condron R, Thomas I, Polya GM (1994) Purification and sequencing of a family of wheat lipid transfer protein homologoues phosphorylated by plant calcium-dependent protein kinase. Biochim Biophys Acta **1209:** 183–190

Pyee J, Yu H, Kolattukudy PE (1994) Identification of a lipid transfer protein as the major protein in the surface wax of broccoli leaves. Arch Biochem Biophys **331:** 460–468

Reggiori F, Klionski DJ (2002) Autophagy in the eukaryotic cell. Eukaryotic Cell **1:** 11–21

Schmid M, Simpson D, Gietl C (1999) Programmed cell death in castor bean endosperm is associated with the accumulation and release of a cysteine endopeptidase from ricinosomes. Proc Natl Acad Sci USA **96:** 14159–14164

Segura A, Moreno M, Garcia-Olmedo F (1993) Purification and antipathogenic activity of lipid transfer proteins (LTPs) from the leaves of *Arabidopsis* and spinach. FEBS Lett **332:** 243–246

Shevchenko A, Sunyaev S, Loboba A, Shevchenko A, Bork P, Ens W, Standing KG (2001) Charting the proteomes of organisms with unsequenced genomes by MALDI-Quadrupole time-of flight mass spectrometry and BLAST homology searching. Anal Chem **73:** 1917–1926

Shevchenko A, Wilm M, Vorm O, Mann M (1996) Mass spectrometric sequencing of proteins from silver stained polyacrylamide gels. Anal Chem **68:** 850–858

Shewry PR, Napier JA, Tatham AS (1995) Seed storage proteins: structures and biosynthesis. Plant Cell **7:** 945–956

Sterk P, Booij K, Schellekens GA, van Kammen A, de Vries SC (1991) Cell-specific expression of the carrot EP2 lipid transfer protein gene. Plant Cell **3:** 907–921

Subirade M, Salesse C, Marion D, Pezolet M (1995) Interaction of a nonspecific wheat lipid transfer protein with phospholipid monolayers imaged by fluorescence microscopy and studied by infrared microscopy. Biophys J **69:** 974–988

Takahashi A, Kawasaki T, Henmi K, Shii K, Kodama O, Satoh H, Shimamoto K (1999) Lesion mimic mutants of rice with alterations in early signaling events of defence. Plant J **17:** 535–545

Tchang F, This P, Stiefel V, Arondel V, Morch MD, Pages M, Puigdomenech P, Grellet F, Delseny M, Buillon P et al. (1988) Phospholipid transfer protein: full-length cDNA and amino acid sequence in maize. J Biol Chem **263:** 16849–16856

Thoma S, Hecht U, Kippers A, Botella J, de Vries S, Somerville C (1994) Tissue-specific expression of a gene encoding a cell wall-localized lipid transfer protein from *Arabidopsis*. Plant Physiol **105:** 35–45

Thompson JD, Gibson TJ, Plewniak F, Jeanmougin F, Higgins DG (1997) The CLUSTAL_X windows interface: flexible strategies for multiple sequence alignment aided by quality analysis tools. Nucleic Acids Res **25:** 4876–4882

Towbin H, Staehelin T, Gordon J (1979) Electrophoretic transfer of proteins from polyacrylamide gels to nitrocellulose sheets: procedure and some applications. Proc Natl Acad Sci USA **76:** 4350–4354

Tsugita A, Kamo M (1999) 2-D electrophoresis of plant proteins. *In* AJ Link, ed, Methods in Molecular Biology, Vol 112: 2-D Proteome Analysis Protocols. Humana Press, Totowa NJ, pp 95–97

Wilm M, Shevchenko A, Houthaeve T, Breit S, Schweigerer L, Fotsis T, Mann M (1996) Femtomole sequencing of proteins from polyacrylamide gels by nano-electrospray mass spectrometry. Nature **379:** 466–469